RESEARCH ARTICLE

ADVANCED HEALTHCARE MATERIALS
www.advhealthmat.de

Topical Nanoliposomal Collagen Delivery for Targeted Fibril Formation by Electrical Stimulation

Albertus Ivan Brilian, Sang Ho Lee, Agustina Setiawati, Chang Ho Kim, Soo Ryeon Ryu, Hyo-Jin Chong, Yejin Jo, Hayan Jeong, Bong-Gun Ju, Oh-Sun Kwon, Giyoong Tae, and Kwanwoo Shin**

Collagen is a complex, large protein molecule that presents a challenge in delivering it to the skin due to its size and intricate structure. However, conventional collagen delivery methods are either invasive or may affect the protein's structural integrity. This study introduces a novel approach involving the encapsulation of collagen monomers within zwitterionic nanoliposomes, termed Lip-Cols, and the controlled formation of collagen fibrils through electric fields (EF) stimulation. The results reveal the self-assembly process of Lip-Cols through electroporation and a pH gradient change uniquely triggered by EF, leading to the alignment and aggregation of Lip-Cols on the electrode interface. Notably, Lip-Cols exhibit the capability to direct the orientation of collagen fibrils within human dermal fibroblasts. In conjunction with EF, Lip-Cols can deliver collagen into the dermal layer and increase the collagen amount in the skin. The findings provide novel insights into the directed formation of collagen fibrils via electrical stimulation and the potential of Lip-Cols as a non-invasive drug delivery system for anti-aging applications.

1. Introduction

Collagen, a key component of the extracellular matrix (ECM) predominantly found in the dermis of the skin, is well-known for its role in the strength and elasticity of the skin.[1] However, delivering and anchoring this large and complex protein molecule to the skin, particularly to the dermis, with the aim of restoring elasticity or preventing wrinkles, is known to pose a significant challenge.[2] Delivering collagen holds medical significance as well, in close proximity to the skin, contributing to the repair of dermal tissues, promoting wound healing, and supporting overall skin health.[3] Traditional methods, such as direct collagen deposition through dermal filler injection, are invasive and carry a risk of infection and allergic reactions.[4] Reducing collagen size through hydrolysis methods may compromise its structural integrity and diminish its effectiveness compared to intact collagen.[5] Therefore, delivering collagen in its monomer form through the skin's outermost layer is essential. To improve the delivery of collagen, nanocarriers have emerged as a promising alternative.[6] Nanostructured drug delivery systems can maintain the stability of molecules and enhance their solubility and diffusion coefficient within the stratum corneum. Among the most widely used nanocarriers are liposomes, which are vesicles composed of phospholipid bilayers enclosing an aqueous compartment that can hold hydrophilic molecules.

The application of electric fields (EF) in transdermal and topical drug administration has demonstrated positive effects in accelerating medical outcomes.[7] EF application exhibits the capacity to diminish the resistance of stratum corneum, facilitating enhanced penetration of EF into the deeper layer of the skin, thereby optimizing the effective permeation of drugs. Simultaneously, EF has been known for its influence on the process of collagen fibrillogenesis, which involves the self-assembly of protein fibers in its interface.[8] EF is observed to affect the alignment and aggregation of collagen monomers, promoting the formation of highly ordered and oriented fibrils.[9] This process is thought to be due to the net charge of collagen monomers, which makes them sensitive to electric fields.[10] In cosmetic applications, such as skin rejuvenation and wrinkle reduction, electric fields have been also proposed to promote the expression

A. I. Brilian, S. H. Lee, A. Setiawati, C. H. Kim, S. R. Ryu, O.-S. Kwon, K. Shin
Department of Chemistry and Institute of Biological Interfaces
Sogang University
35 Baekbeom-ro, Mapo-gu, Seoul 04107, Republic of Korea
E-mail: kwshin@sogang.ac.kr

A. Setiawati
Faculty of Pharmacy
Sanata Dharma University
Paingan, Maguwoharjo, Depok, Sleman, Yogyakarta 55284, Indonesia

H.-J. Chong, Y. Jo, H. Jeong, B.-G. Ju
Department of Life Science
Sogang University
35 Baekbeom-ro, Mapo-gu, Seoul 04107, Republic of Korea

G. Tae
School of Materials Science and Engineering
Gwangju Institute of Science and Technology
123 Cheomdangwagi-ro, Buk-gu, Gwangju 61005, Republic of Korea
E-mail: gytae@gist.ac.kr

The ORCID identification number(s) for the author(s) of this article can be found under https://doi.org/10.1002/adhm.202400693

DOI: 10.1002/adhm.202400693

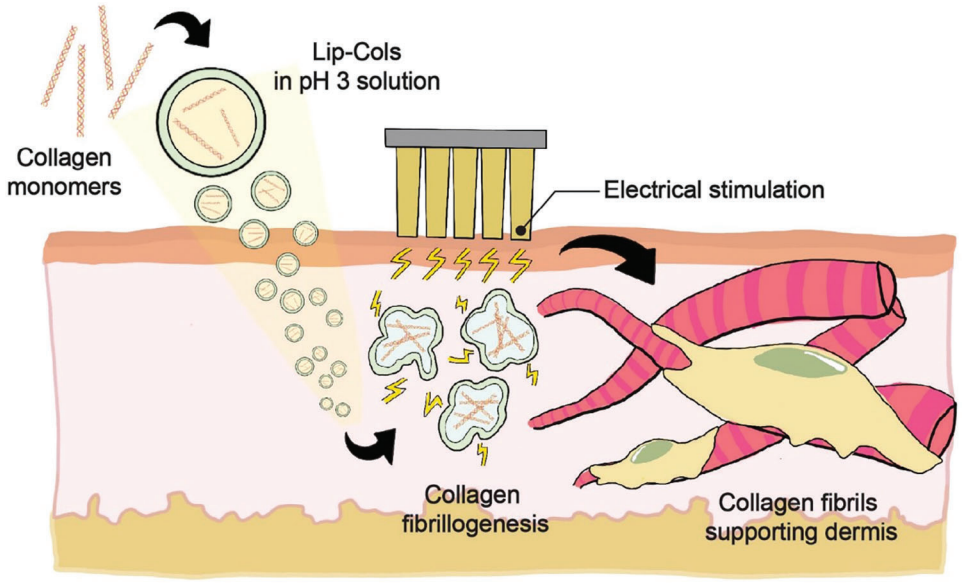

Figure 1. Schematic illustration of the encapsulation of collagen monomers in the acidic microenvironment of nanoliposomes and the subsequent application of Lip-Cols onto the skin, followed by electric fields. This process is designed to promote the formation of collagen fibrils within the dermal layer of the skin.

of collagen and elastin in human dermal fibroblast (HDF) cells, which are responsible for producing ECM in the skin.[11]

Nevertheless, in order to better utilize EF for wrinkle reduction or the restoration of skin elasticity by using external collagen, the following challenges must be addressed. First, collagen monomers at the molecular level need to be externally delivered, passing through the epidermis to reach the dermis. In other words, externally applied collagen monomers should only self-assemble into fibrils, underneath the skin, particularly in the dermal layer. Thus far, a collagen delivery system achieving fibrilization exclusively in the dermis region has not been reported. We posit that if effective delivery of collagen monomers is possible, EF could be utilized as an external stimulus inducing localized fibrillogenesis in this collagen delivery system.

In this study, we report a novel approach involving the synergistic combination of zwitterionic charge nanoliposomes (NLs) for collagen encapsulation and the concurrent application of electrical stimulation to regulate collagen fibrillogenesis and facilitate topical collagen delivery. Our findings show that by using minimal induction of EF, such as an alternating current (AC) with a frequency of 10 Hz and a voltage of 1 V, these collagen-encapsulated nanoliposomes (Lip-Cols) can be directed effectively to self-organize and form structural collagen fibers in situ (**Figure 1**). Considering that the monomeric form of collagen is highly sensitive to pH changes,[12] our approach involved creating an acidic microenvironment inside the NLs to maintain collagen in its monomer form. Utilizing real-time imaging techniques, we captured the dynamic process of collagen fibril formation facilitated by Lip-Cols under the influence of EF, providing insight into the self-assembly process. Furthermore, we demonstrated the impact of Lip-Cols and EF on collagen fibrils orientation and their permeability properties in vitro and in vivo. With the application of electrical stimulation, our Lip-Cols have the potential as a drug delivery system for skin rejuvenation by depositing collagen monomers and forming collagen fibrils as structural support.

2. Results and Discussion

2.1. Lip-Cols Characterization

In order to effectively deliver drugs or bioactive compounds through the skin's stratum corneum layer, it is important to consider liposome properties such as particle size and lipid composition.[13] Prior to the encapsulation process of collagen monomers, a 200-nm polytetrafluoroethylene polymer (PTFE) membrane was used to filter the collagen solution. Atomic force microscopy (AFM) imaging and dynamic light scattering were used to observe the collagen solution before and after the membrane filtration process, as shown in Figure S1a,b, Supporting Information. The pre-filtration collagen solution was observed to have a mean diameter of 855 ± 124 nm and polydispersity index (PDI) of 0.68 ± 0.09. The post-filtration mean diameter of collagen monomers was 87 ± 7 nm with smaller PDI (0.14 ± 0.01) compared to without filtration. The filtered collagen was then encapsulated within zwitterionic:cholesterol (9.5:0.5) NLs using a gentle-hydration method to produce Lip-Cols with mean diameter of 223 ± 2 nm and PDI value of 0.12 ± 0.03, as shown in Figure S1c, Supporting Information. The low PDI values (<0.18) indicated the homogeneity in the particle size distribution of Lip-Cols. The drug-loading content (DLC%) of Lip-Cols was 3.4 ± 0.1 and the encapsulation efficiency (EE%) was measured to be 16.9 ± 0.6 through a comparison of the fluorescent intensity before and after the separation of Lip-Cols from its supernatant, as demonstrated in Figure S1d, Supporting Information. Previous research conducted by Phan et al.[14] showed that negatively charged phosphatidylserine promoted collagen-binding on the membrane surface of giant unilamellar vesicles,

and spontaneous fibril formation occurred when the outer solution changed to a neutral pH solution. The zeta potential measurement revealed that Lip-Cols exhibited a surface charge of +4.4 mV (Table S1, Supporting Information). Neutral-charged phosphatidylcholine minimized collagen binding on the nanoliposome surface, and the acidic microenvironment inside the nanoliposome could hinder collagen fibril formation due to the electrostatic repulsion.[15] Additionally, cholesterol in the lipid mixture improved bilayer characteristics by increasing membrane fluidity, reducing permeability to water-soluble molecules, and improving bilayer stability.[16]

2.2. Collagen Fibril Formation from Lip-Cols Stimulated by Electric Fields

The utilization of electric fields has been documented in manipulating protein such as to open or unfold the protein structure, to control the orientation of surface-bound peptides and surface concentration.[17] Diverse measurements, platforms, and electrical components have been introduced to demonstrate the capability of electric fields.[8,18] Here, we demonstrated the ability of low EF to guide the assembly of Lip-Cols using an AC field with a frequency of 10 Hz and a voltage of 1 V. To set up the EF stimulation, a home-built reactor with a chamber was connected to two electrodes, which were then connected to a function generator to apply an AC electric current, as illustrated in Figure S2, Supporting Information.

The real-time fibrillogenesis process of Lip-Cols was observed under a confocal microscope, as shown in **Figure 2**. Following encapsulation, Lip-Cols were exposed to the EF and observed on the electrode interface, as depicted in Figure 2a. Selected events from Movies S1a and S1b, Supporting Information showed the formation of collagen fibrils from Lip-Cols under EF in real-time, as shown in Figure 2b. In the absence of electric fields, as a control, Lip-Cols were dispersed in the solution and presented as yellow color due to the colocalization of TopFluor-labeled NLs and Alexa 647-labeled collagen. In the presence of electric fields, Lip-Cols migrated and formed a large aggregation within five min (white arrow). Alignment toward the electrode was observed in the eleventh min (white arrows) and continued to grow, as more Lip-Cols aligned toward the electrode in the fortieth min. The migration and alignment of Lip-Cols toward the electrodes resulted in a significant decrease in fluorescence, as quantified in Figure 2c. Collagen monomers inside nanoliposomes responded to electrophoretic flow generated by EF, which was facilitated by the acidic solution in which they were fully protonated.[19] Simultaneously, the EF-triggered electroporation and fusion process between liposomes led to aggregation between Lip-Cols.[20] Once this aggregation occurred, collagen monomers could interact and assemble into fibrils[21] as shown in Figure 2d, Lip-Cols exhibited a matrix-like morphology, and a long fibril-like shape after 1 h of electrification. Transmission electron microscopy (TEM) image of Lip-Cols after exposure to EF revealed a similar matrix-like morphology, as observed in the confocal microscopy observations, with fibril diameters ranging from 33 to 73 nm (Figure 2e). A notable contrast was observed between the behavior of bare liposomes and Lip-Cols following the exposure of EF. As depicted in Figure S3, Supporting Information, bare liposomes exhibited aggregation at the electrode interface and dispersed within the aqueous medium. Differently, Lip-Cols that formed a matrix-like structure remained intact on the electrode surface.

2.3. Self-Assembly of Collagen Monomers under Electric Fields

To investigate the process of fibrillogenesis in Lip-Cols, we performed experiments in collagen solution and examined the self-assembly of collagen monomers under the influence of EF, as depicted in **Figure 3**. Two electrodes were inserted into a 0.01 M hydrochloride (HCl) solution with pH 3, containing Alexa 647-labeled collagen, and the self-assembly process was monitored at the electrode interface in real-time using confocal microscopy, as shown in Figure 3a. Representative confocal images from Movies S2a and S2b, Supporting Information demonstrated that initially, in the "OFF" condition, there were no collagen fibrils or aggregates, as collagen remained in its monomeric form in the acidic environment (Figure 3b). Upon application of the AC electric current to the electrodes, collagen monomers started migrating, and aggregation began in as little as 10 s. A noticeable change in fluorescent intensity was observed in less than 1 min at the electrode interface (white arrow). The branching assembly of collagen fibrils was observed at four min and continued to form collagen networks with longer exposure as presented at fifteen min (white arrows). Similar to Lip-Cols fibrillogenesis, a significant decrease in fluorescent intensity measured at the electrode interface resulted from the migration and alignment of collagen monomers into fibrils and, eventually, fibers (Figure 3c). TEM images of collagen exposed to EF at various time intervals corroborated the findings from confocal microscopy observations. No fibers were evident in collagen at pH 3. However, fibrils with diameters ranging from 28 to 70 nm emerged within 9 min of the initiation of electrical stimulation. Subsequently, as the duration of electrical stimulation increased (≈15 min), long fibers and sizable collagen aggregates were observed (Figure 3d).

Under two different charged electrodes, namely positive and negative electrodes, the formation of collagen fibrils was observed from both electrodes and converged at the middle of both electrodes (white arrows) (Figure S4a, Supporting Information). Furthermore, in the presence of EF, collagen self-assembly was initiated from the working electrode ("ON") and progressed toward the not-working electrode (″OFF) in a directed manner, as evidenced by the change in fluorescent intensity (white arrows) (Figure S4b, Supporting Information). The resulting collagen fibrils were observed to attach to both negatively charged cathode and positively charged anode. Differently, Huelin et al.[8] reported that no collagen near the counter electrode (positively charged) in the hull cell system, after 30 min of electrification. The location of fibril assembly appeared to be influenced by the distance between the electrodes, with closer proximity leading to aggregation around the electrodes despite of charge.

2.4. Collagen pH Gradient and Structural Conformation Changes under Electric Fields

The observation that collagen fibrils are formed by EF in a low-pH environment, where monomers typically do not self-assemble into collagen fibrils,[12] prompts us to hypothesize that

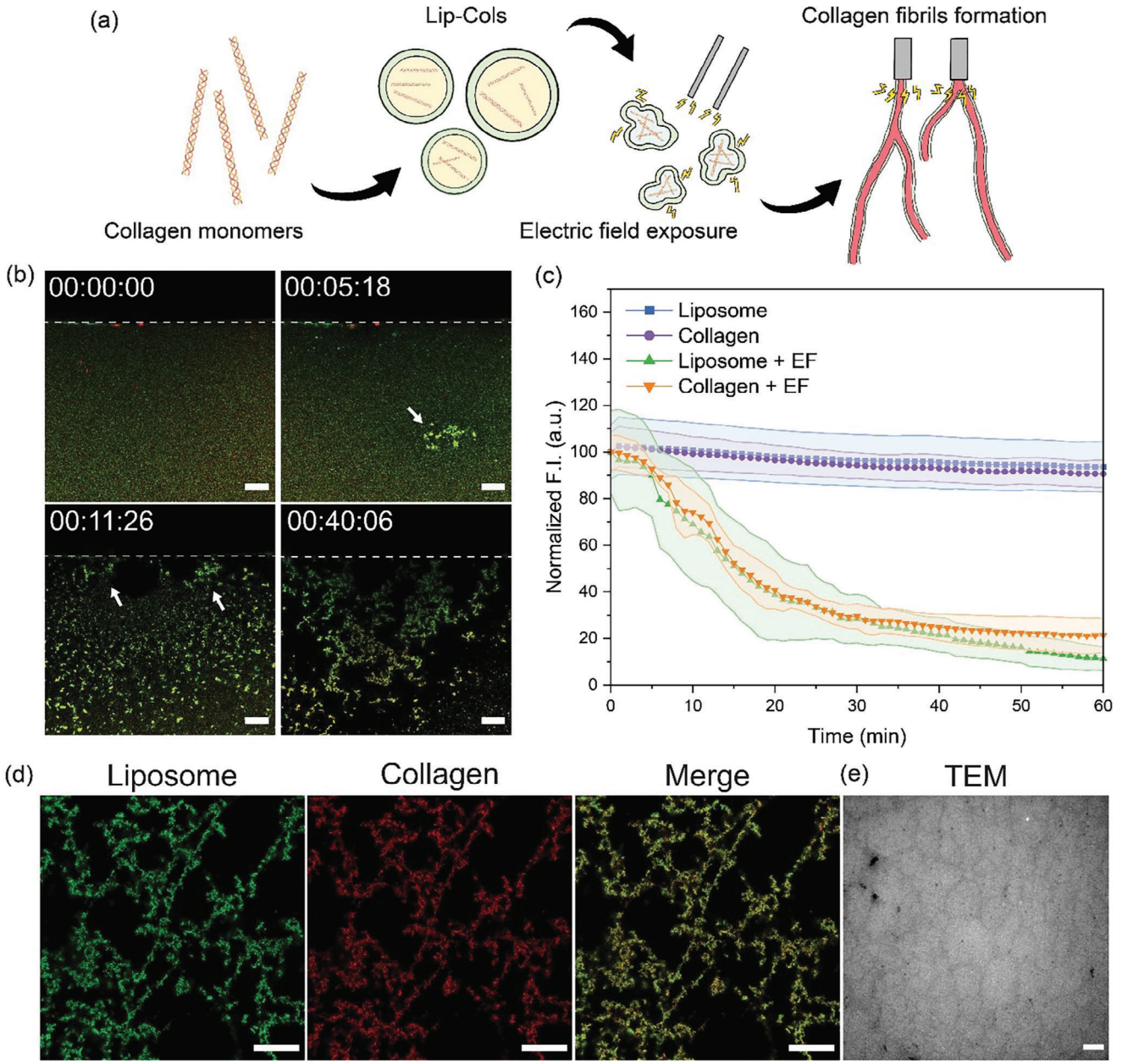

Figure 2. Collagen fibril formation from Lip-Cols under EF. a) Schematic illustration of collagen fibril formation from Lip-Cols under EF. b) Representative confocal images of the formation of collagen fibrils from Lip-Cols at electrode interface under EF in time-dependent. Dash line is the electrode and the white arrows show Lip-Cols aggregation. c) Time-dependent changes in fluorescence intensity of Lip-Cols at electrode interface under EF and without exposure. d) Confocal and e) TEM images of collagen fibrils from Lip-Cols after 1 h of EF exposure. The green color is nanoliposome and the red color is collagen. The scale bar of (b) is 30 μm, and that of (d) and (e) is 25 μm.

an electrical stimulus, like EF, may induce a localized pH change. This pH alteration could trigger the instantaneous transition of monomers into an environment conducive to the spontaneous polymerization of collagen.[22] Therefore, we investigated the change of pH gradient (ΔpH) and confirmed the changes in collagen structural conformation before and after EF as depicted in **Figure 4**. We measured the ΔpH solution of HCl, collagen-only, liposome-only, and Lip-Cols while EF was applied (Figure 4a). The pH of the solution began to oscillate upon EF application due to the electrochemical oscillation process.[23] In HCl and liposome-only solution, there was a negative ΔpH change and it returned to the initial state once the EF was stopped. In contrast, the ΔpH of collagen-only solution showed a positive trend, where the ΔpH increased to 0.16 ± 0.01 points from the initial state after the electrodes were turned off. In Lip-Cols solution, the ΔpH was decreased, and it increased to 0.13 ± 0.01 points from the initial state after EF. The migration of collagen monomers under the influence of EF resulted in changes to their

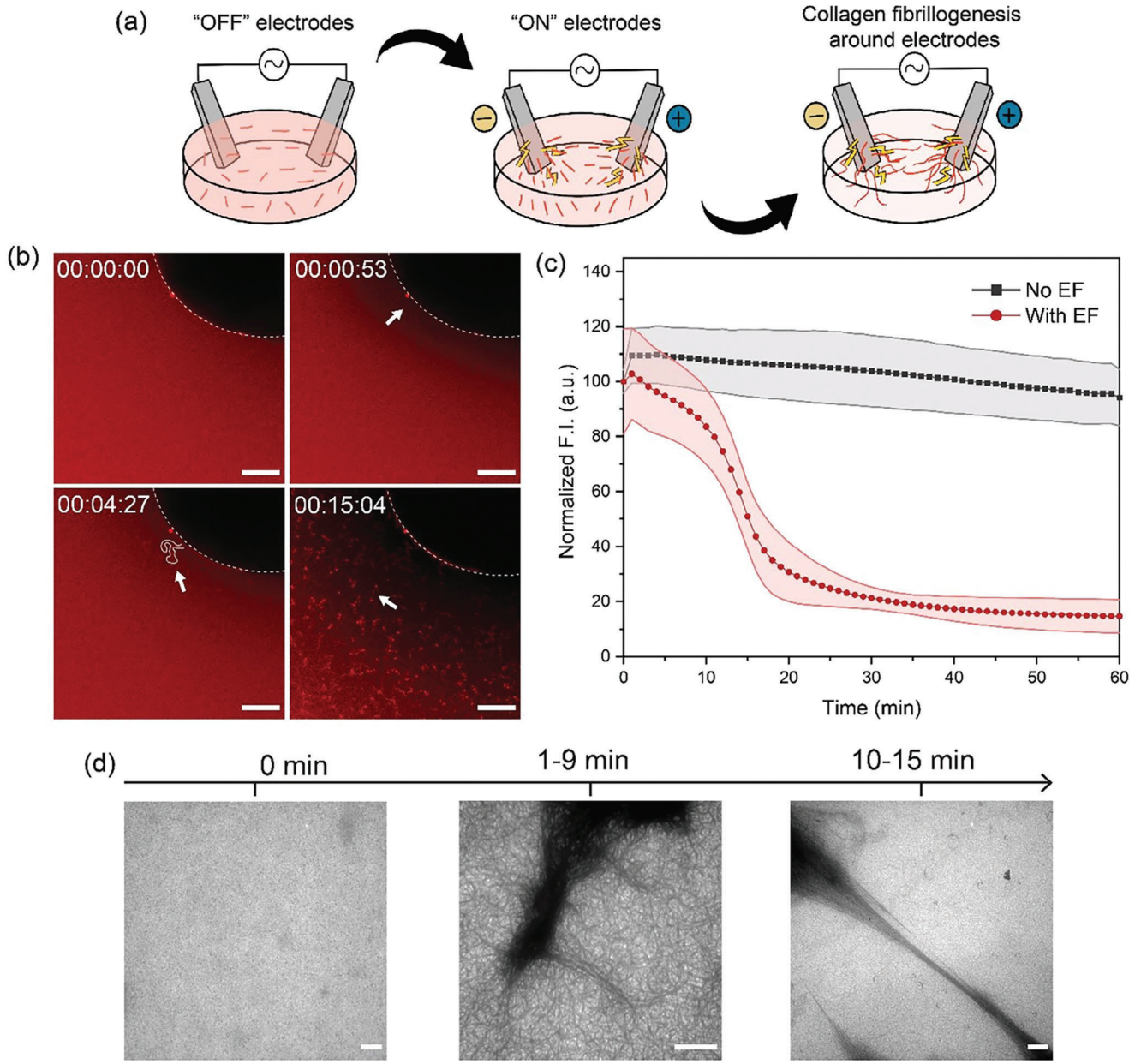

Figure 3. Self-assembly of collagen monomers under electric fields. a) Schematic of collagen fibrillogenesis between two different electrodes. b) Representative confocal images of the formation of collagen fibrils under EF in time-dependent. Dash line is the electrode and the white arrows show the formation process of collagen fibrils. c) Time-dependent changes in the fluorescence intensity of collagen monomers under EF and without the exposure. d) TEM images of collagen at different times under EF. The red color is collagen. The scale bar of (b) is 30 μm, and that of (d) is 1 μm.

net charge, eventually becoming net neutral at their isoelectric point.[24]

The structural changes of collagen from monomeric to fibrillar forms were evaluated using circular dichroism (CD) and Fourier-transform infrared spectroscopy (FT-IR) analysis, as presented in Figure 4b,c. In pH 3 HCl solution, the collagen CD spectrum exhibited a negative peak at around 197 nm and a positive peak at 221 nm, indicating the triple helical structure of collagen.[25] In a neutral pH buffer, a slight shift of the negative peak from 197 to 199 nm and the positive peak from 221 to 222 nm was observed. Upon exposure to electrical stimulation, a negative peak shift toward neutral pH, an increase in negative peak intensity, and a decrease in positive peak intensity were observed, indicating a tendency toward collagen in a neutral pH solution. The exposure of native collagen to EF resulted in the gradual loss of its stability, as evidenced by changes in the CD spectra.[26] FT-IR spectra of collagen before EF exposure exhibited amide I, amide II, and amide III bands at 1654, 1550, and 1240 cm^{-1}, respectively.[27] After electrical stimulation, a reduction of Amide I intensity was observed, leading to a shift in the amide I/II ratio. The changes in the Amide I/II ratio altered the polarization of collagen monomers and the orientation of fibrils from the amide carbonyls (0°) to the

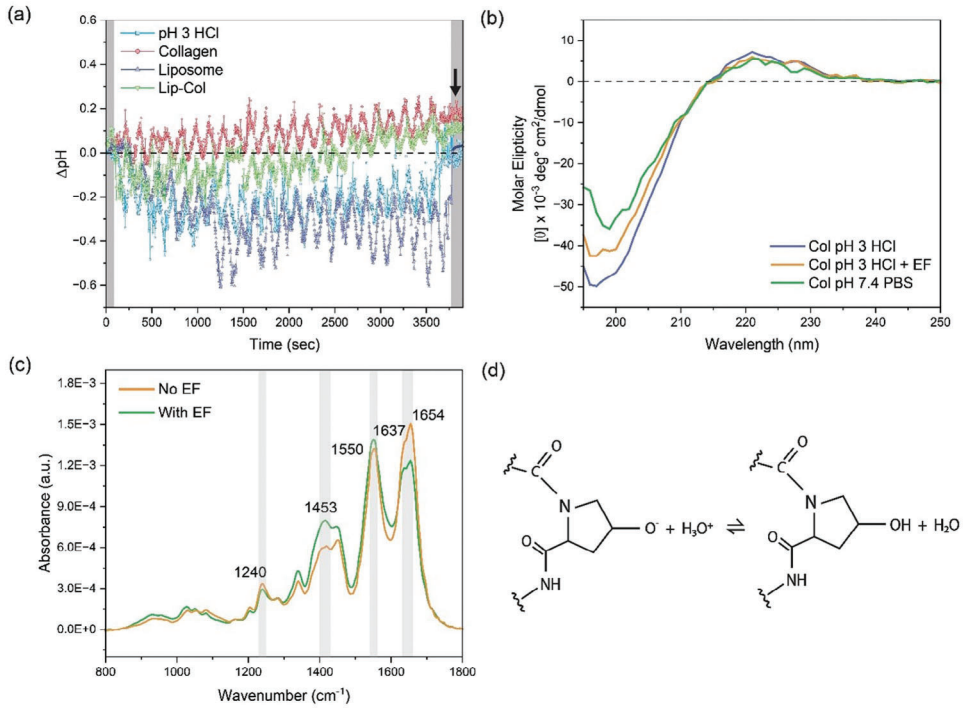

Figure 4. Collagen pH gradient and structural conformation changes under electric fields. a) the ΔpH change of HCl solution, collagen, liposome, and Lip-Col solution under EF. The grey areas indicate the absence of EF and the white area indicates the presence of EF. The black arrow indicates the final ΔpH after electrical stimulation. b) CD spectrum of collagen in pH 3 HCl solution (blue), after electrical stimulation (orange), and PBS (green). c) FT-IR spectrum of collagen monomer before (orange) and after (green) stimulated with EF. d) Interaction of O^- group of hydroxyproline amino acid in the peptide chains of collagen fibrils with hydronium ion and formation of the water molecule.

backbone (90°).[28] The observed alteration in the Amide I band ratio of 1654/1637 cm^{-1} signified an augmentation in β-sheets and a concurrent decrease in α-helices, attributed to protein aggregation and fiber bundling.[29] Concurrently, an enhancement of pyrrolidine rings of proline and hydroxyproline side chains band (1453 cm^{-1}) was noted. The change in ΔpH solution in collagen-only and Lip-Cols under EF was possibly triggered by the electrical interaction between hydronium ion and hydroxyl group of hydroxyproline amino acid in the peptide chains of collagen, resulting in the formation of water molecules and hydroxide group of collagens (Figure 4d).[30] The EF could decrease the electrostatic repulsion and alter the net charge density of collagen monomers, enabling interaction between the O^- group of hydroxyproline amino acid and hydronium ions, resulting in the formation of water molecules that changed the pH gradient of the solution.

2.5. Lip-Cols Influence Collagen Fibril Orientation on HDFs

The question arises as to whether collagen fibrils induced by electrical stimulation exhibit properties similar to fibrils formed in the free environment in the extracellular region of the cell. Subsequently, we investigated whether collagen assembled in a directional electric field would demonstrate a similar anisotropic orientation around cultured cells as observed at the electrodes. In examining the cellular interaction of Lip-Cols, we revealed distinct collagen fibril orientations between the collagen-treated group and Lip-Cols-treated group (with or without EF), as illustrated in **Figure 5**a. Fluorescently labeled collagen, NLs, and Lip-Cols were exposed to HDF cells for 1 h and EF was subjected to Lip-Cols + EF-treated group solution at the same interval. Following the incubation, HDF cells underwent washing with phosphate buffer saline (PBS), preserving the orientation and accumulation of the samples within the cells, as shown in Figure 5b. The directionality of the fibrils toward HDFs was quantified, and the angular distribution of fibrils was plotted and fit to a Gaussian model (Figure 5c). Fibroblasts treated with collagen exhibited a collagen fibril matrix with a random orientation on the cell surface, where the collagen direction was oriented to −67° and the cell was oriented to 2°. Conversely, the Lip-Cols-treated group showed a collagen matrix aligned with the orientation of HDFs, directed at 12° and 11° for collagen fibrils and cells, respectively. The alignment of collagen exhibited an orientation toward the cell's morphology, suggesting a correlation between collagen alignment and the shape of the cell, guided by the presence of NLs. Exposing HDFs to EF during Lip-Cols incubation, induced a minor shift in the alignment of collagen fibrils on the cells. Specifically, the collagen fibrils exhibited an orientation of 14°, while the cells were oriented to 25°.

The orientation of collagen fibers has been reported to influence cell-ECM interactions and cell differentiation.[31] The observed lack of alignment in collagen fibers toward HDFs can be attributed to the abrupt fibrillogenesis of collagen monomers, prompted by variations in pH and ionic strength of the cell culture medium. NLs played a crucial role in protecting collagen

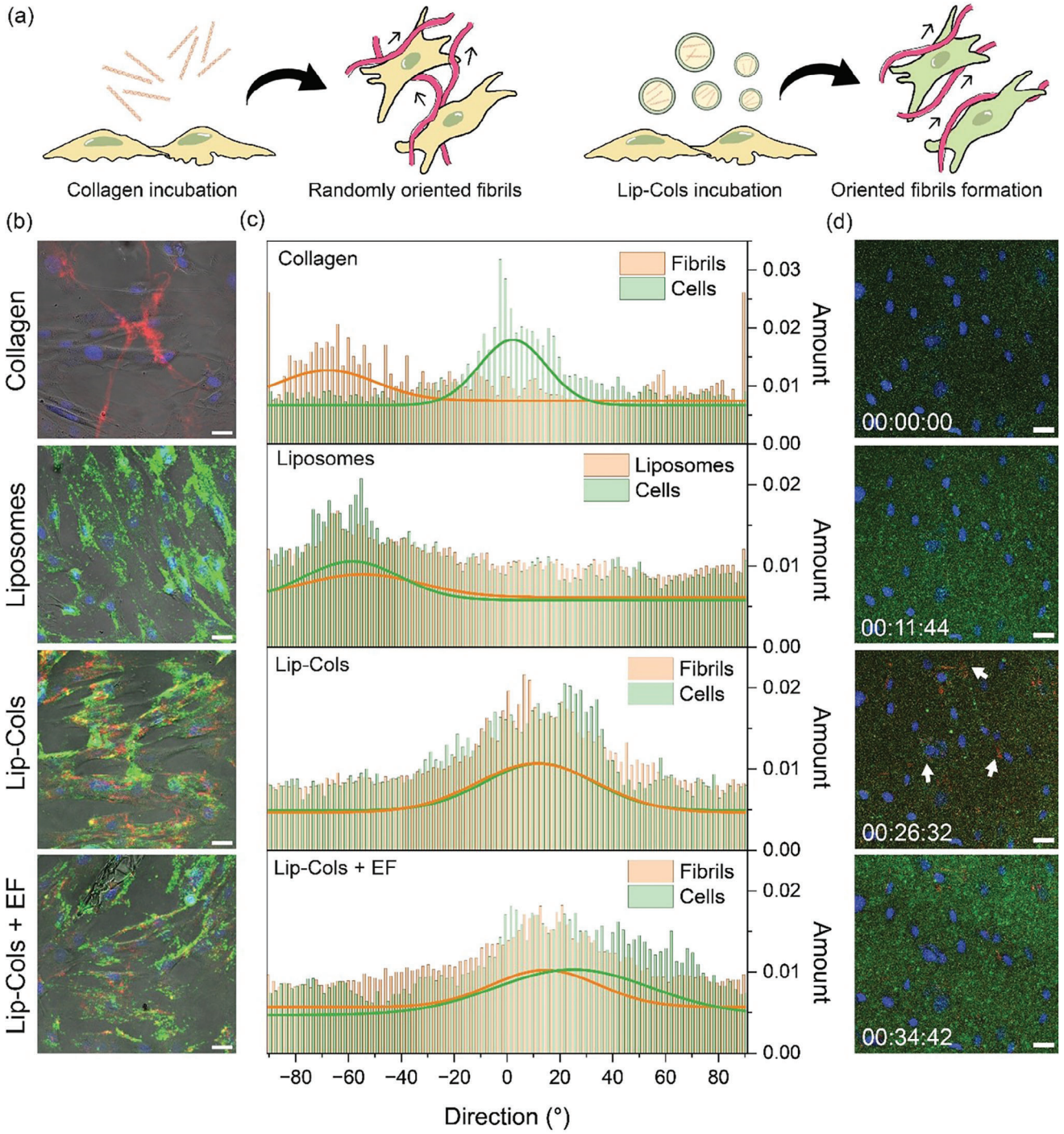

Figure 5. The orientation of collagen fibrils and the cellular interaction of Lip-Cols under electric fields. a) Schematic illustration of collagen fibrils orientation following incubation with either collagen or Lip-Cols. b) Confocal images of HDFs subsequent to sample incubation, accompanied by c) a directionality analysis of collagen fibrils and cells. Nuclei are depicted in blue, collagen in red, liposomes in green, and cells in gray. d) The real-time cellular uptake of Lip-Cols under electric fields, with white arrows highlighting collagen fibrils in HDFs. The scale bar of (b) and (d) is 30 μm.

monomers, ensuring their delivery to the cell surface for the establishment of a collagen matrix. The minor alteration in the alignment of collagen fibrils observed in the Lip-Cols + EF-treated group was attributed to the influence of EF. The application of EF facilitated the distribution of collagen fibers on HDF cells and governed the formation of collagen fibrils. The EF exposure induced oscillations in the culture medium, generating waves, as evidenced by live cell imaging presented in Movie S3, Supporting Information and Figure 5d. Initially, the green fluorescence from NLs was observed, and upon exposure to EF,

Lip-Cols were propelled in a wave-like manner, interacting with HDF cells (eleventh min). Subsequently, collagen fibrils began to appear and accumulate, as indicated by the white arrows in the 26th minute and continued by the second wave of Lip-Cols that was observed in the 34th minute.

2.6. Lip-Cols and EF Enhance the Permeability of Collagen Monomers in Skin Layers

To simulate the in vitro condition of the skin and investigate the permeability of Lip-Cols, we designed a skin-like experiment using a transwell system.[32] The skin-like transwell included two compartments: a layer of human keratinocyte (HaCaT) cells in the transwell insert that simulated the epidermis layer, and a layer of HDF cells in the plate well that simulated the dermis layer, as illustrated in Figure S5a, Supporting Information. To confirm the formation and attachment of the HaCaT cell layer, we stained the cell seeded-polycarbonate membrane of the transwell insert with hematoxylin and eosin (H&E). The keratinocyte cell layer stained with H&E showed a dark layer, while the membrane without cells showed a bright layer with a polycarbonate structure under the light microscope (Figure S5b, Supporting Information). The equivalency of keratinocyte cell layer conditions was assessed using a fluorescent dye mixed medium on three transwell membranes. Figure S5c, Supporting Information illustrates a consistent fluorescence intensity measured in the plate well of the transwell system, suggesting a uniform formation of HaCaT cell layers.

After preparing the HaCaT and HDF cell layers, Lip-Cols were dropped into the transwell insert, and the permeability of Lip-Cols was assessed after incubation, as depicted in **Figure 6a**. We exposed the HaCaT layer to a concentration of 150 μg mL^{-1} and the level of collagen-conjugated fluorescent in the HDF cell monolayer was measured in a time-dependent experiment, revealing a linear trend between the fluorescent intensity of collagen and prolonged incubation times for Lip-Cols (Figure 6b). Compared to collagen-only, Lip-Cols exhibited a higher permeability effect, as demonstrated in the confocal images of collagen fluorescence (red color) based on the incubation time (Figure 6c). The paracellular route was potentially used by Lip-Cols to traverse the artificial epidermis layer, which involves Lip-Cols passing through the tight junctions between adjacent HaCaT cells.[33] The fluorescence signal was still detected in the HDF cells treated with collagen-only, with no significant increase after 16 h incubation. When collagen was introduced without NLs, it aggregated in the cell medium, and the collagen fibers were too large to pass through the HaCaT cell monolayer.[34]

We conducted an in vivo experiment using female Institute of Cancer Research (ICR) mice to investigate the effect of Lip-Cols and EF on the mouse skin, as illustrated in **Figure 7a**. A printed circuit board was designed to connect 25 electrodes with different applied charges (Figure S6a,b, Supporting Information) to deliver a voltage of 1 V and a frequency of 10 Hz onto the skin. A stage was used to immobilize the electrodes, facilitating 1 h-long application of EF onto the mouse skin surface as depicted in Figure S6c, Supporting Information. To enhance the permeability of Lip-Cols in our dermal formulation, 5% (v/v) propylene glycol was incorporated as an enhancer. The permeation of Alexa 647-labeled collagen (0.5 mg mL^{-1}) is visualized in the heatmap presented in Figure 7b, and representative bright field and fluorescence images of the skin for each group are shown in Figure 7c. The initiation of permeation was normalized to the first layer of the epidermis, revealing high fluorescence intensity in the epidermis of the treated groups. Notably, the presence of EF induced increased permeability of labeled collagen in the collagen-treated group, evidenced by higher intensity and deeper collagen penetration. Similarly, Lip-Cols with EF exhibited stronger fluorescence intensity and deeper penetration through the skin compared to Lip-Cols only and collagen solution. The heatmap and the representative fluorescence images of TopFluor-labeled NLs (Figure S7a,b, Supporting Information) revealed slight auto-fluorescence in mouse skin tissue in the non-nanoliposome-treated group. Nevertheless, the auto-fluorescence was distinctive enough to display a higher fluorescence distribution of TopFluor in the Lip-Cols with EF compared to Lip-Cols without electrical stimulation. The previous research on the impact of liposomal surface charge on dermal drug delivery elucidated that neutral liposomes manifested minimal fluorescence in deeper skin strata compared to their anionic or cationic counterparts, yet were suggested to be used in dermal application for their non-irritant property.[35] Zwitterionic liposomes mainly entered cells through both clathrin-independent endocytosis and macropinocytosis.[36]

Quantification of Alexa 647-labeled collagen in the dermis layer (Figure 7d) demonstrated significant differences among groups. Mice treated with collagen with EF (0.51 ± 0.09), Lip-Cols (0.64 ± 0.17) and Lip-Cols with EF (0.89 ± 0.08) showed significant variations compared to the control (0.22 ± 0.08) and collagen-only (0.35 ± 0.03). Collagen-loaded liposomes exhibited superior skin penetration compared to free collagen, resulting in an increased retention of collagen within the skin and consequently delay in its release, consistent with findings from permeability studies conducted by Li et al.[37] The combination of Lip-Cols and EF exhibited a notable permeation ability for delivering collagen, supported by a significant increase of total collagen measured in Lip-Cols + EF (0.39 ± 0.01 μg mg^{-1}) compared to the control group (0.37 ± 0.01 μg mg^{-1}), as shown in Figure 7e. Furthermore, distinct morphologies of labeled collagen were observed in the mouse dermis layer (Figure S8, Supporting Information). The Lip-Cols-treated group exhibited the accumulation of collagen that conformed to the shape of the cell, while the Lip-Cols with EF-treated group displayed a collagen matrix-like structure decorating the dermis layer. HDF cells exhibit bidirectional interaction with collagen orientation, wherein HDF can influence collagen orientation and be driven by the orientation of collagen.[38] In our experimental context, the newly aligned fibrils originating from Lip-Cols could be perceived as a new collagen matrix or subject to remodeling by HDF cells.

The incorporation of collagen with EF group demonstrated the substantial role of EF in promoting collagen penetration into the skin. The application of EF induces a voltage across the skin, eliciting changes in the transmembrane potential of skin cells and transiently creating pores that facilitate the passage of molecules impeded by the skin barrier under normal circumstances.[39] Electroporation induced by EF involves high voltage (>50–300 V) and short-duration pulses.[40] In our study, the application of mild EF, an alternating current of 1 V at 10 Hz for 1 h, was found to

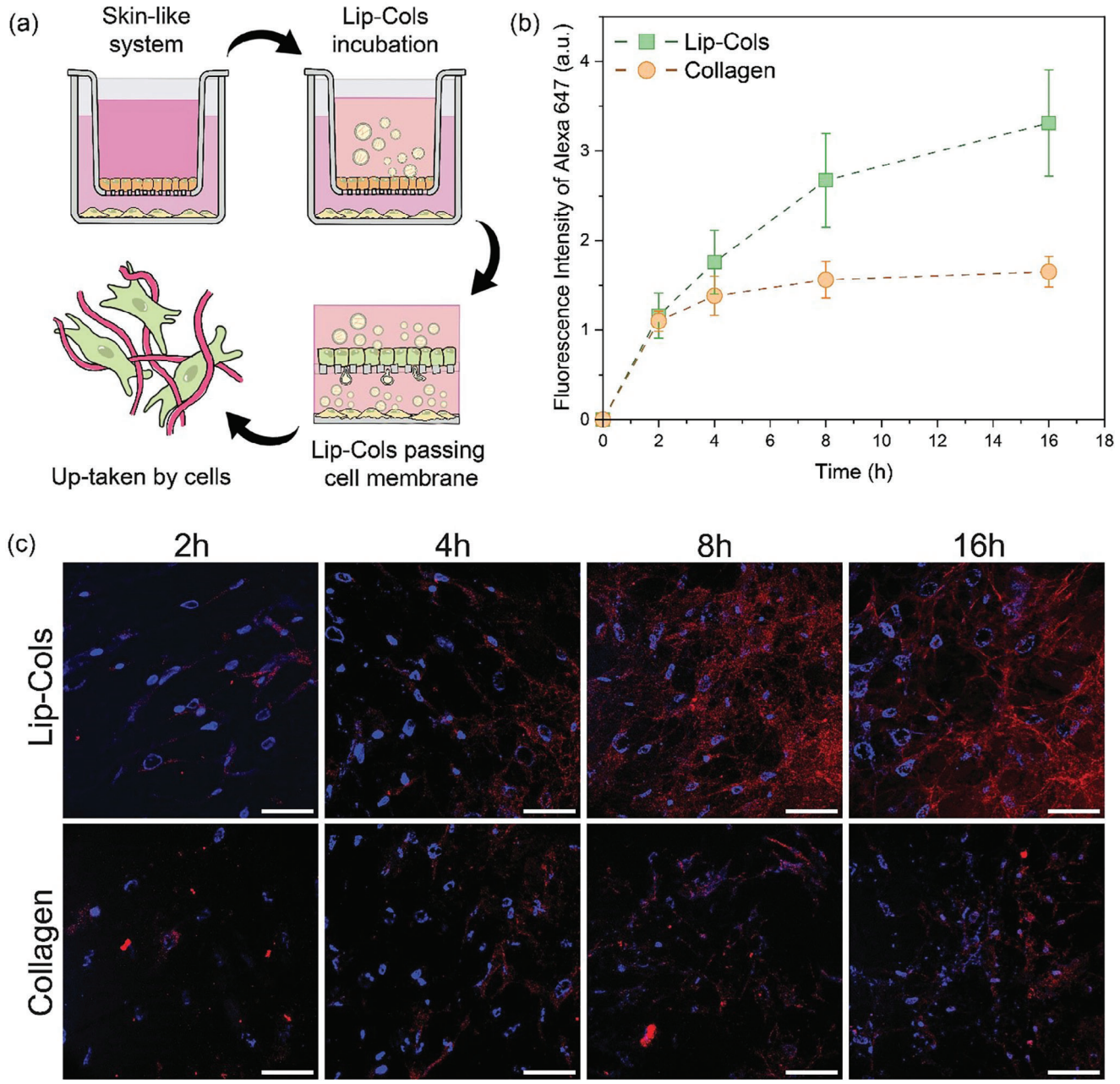

Figure 6. In vitro permeability of Lip-Cols. a) Schematic illustration of cell membrane permeability assay representing the epidermis and dermis layers of skin. b) Fluorescent intensity of Alexa 647-labeled collagen measured in HDF cells at different time points. c) Confocal images of Alexa 647-labeled collagen and DAPI in HDF incubated with Lip-Cols or collagen-only in a skin-like system. The scale bar is 30 μm.

be effective in enhancing the permeability of collagen, whether in its free form or encapsulated within NLs. A study conducted by Li et al. reported that EF could even stimulate dermal collagen production, resulting in a temporally increased fiber density in the skin without the induction of scar formation.[41] Also, a low voltage electrical stimulation (≈2.2 V) was demonstrated to promote wound closure of a full-thickness wound by facilitating fibroblast migration, proliferation, and transdifferentiation.[42] In our experimental condition of applying the mild EF, followed by analysis in 1 day, the contribution of EF itself must be insignificant, considering the minor effect of collagen with EF group. In contrast, the role of EF on the synergistic effect of EF and NLs was significant by enhancing collagen delivery and facilitating fibrillogenesis, thereby forming a collagen matrix in the dermal layer.

3. Conclusions

In this research, we investigated the formation of collagen fibrils from collagen-encapsulated nanoliposomes, or Lip-Cols, through the process of self-assembly guided by EF. The collagen

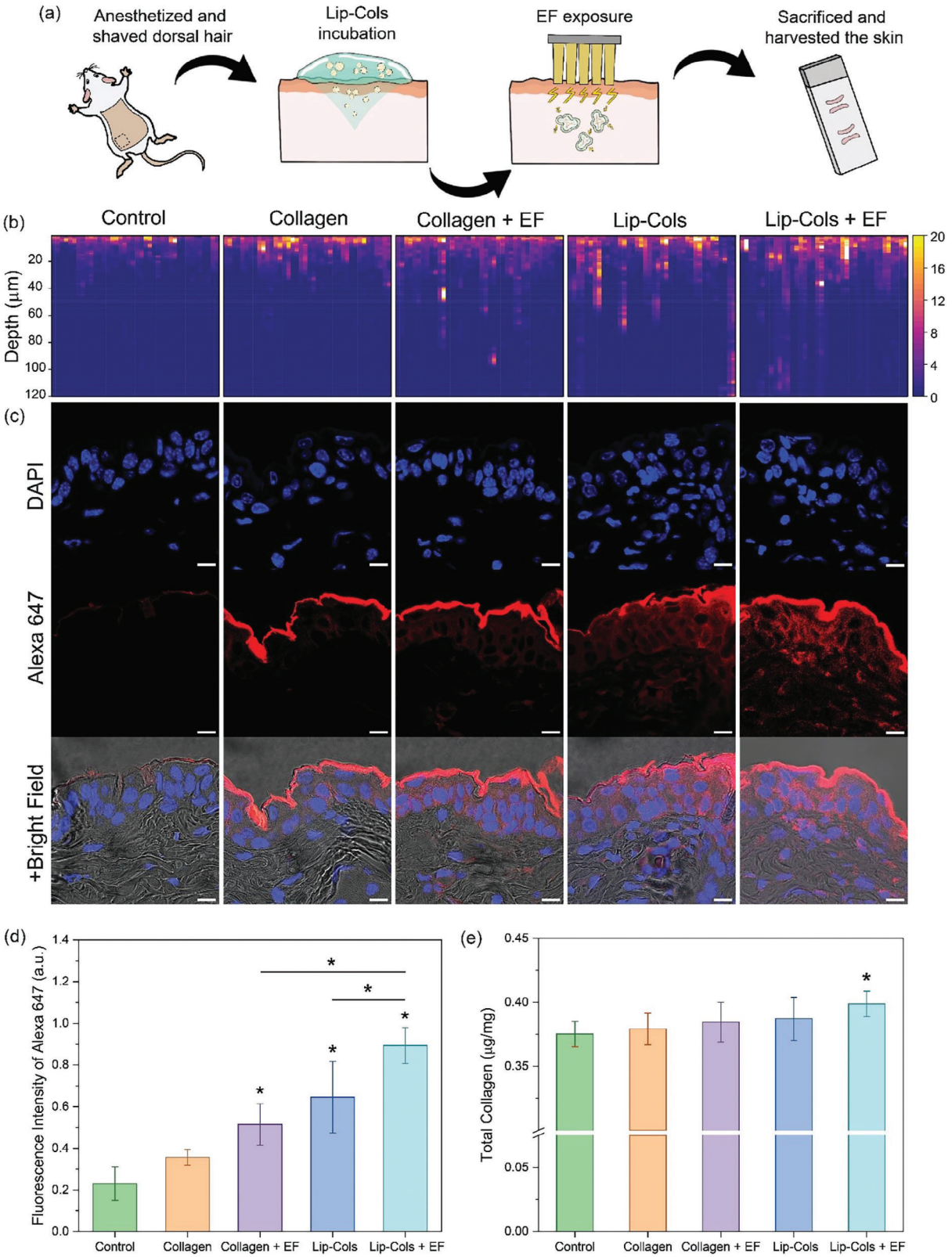

Figure 7. In vivo permeability of Lip-Cols. a) Schematic representation of the Lip-Cols and EF treatment on a mouse model. b) Heatmaps and c) the representative confocal images of Alexa 647-labeled collagen in the cross-section of mouse skin. d) Fluorescent intensity of Alexa 647 labeled collagen in the dermis layer of mouse skin (* $p < 0.05$ in comparison between control and collagen). e) Total collagen amount from skin tissues after treatment with collagen and Lip-Cols, with and without EF ($n = 6$, * $p < 0.05$ in comparison between control). The scale bar is 10 μm.

monomers, which were contained within the zwitterionic NLs and were exposed to an acidic microenvironment, were able to migrate, aggregate, and align into fibrils as a result of electroporation and a pH gradient change under EF. We found that Lip-Cols could penetrate the HaCaT cell monolayer and interact with the cell membrane. In vivo, we demonstrated the impact of EF in augmenting skin permeability and the concurrent application of Lip-Cols and EF exhibited an augmentation in collagen accumulation within the skin. Given that the loss of collagen and collagen fiber integrity are key factors in skin aging, Lip-Cols with electrical stimulation holds great promise as a non-invasive dermatological formulation for rejuvenating and revitalizing skin.

4. Experimental Section

Materials and Reagents: 1,2-dioleoyl-sn-glycero-3-phosphocholine (DOPC), Cholesterol (Chol), and TopFluor-Cholesterol (Top-Chol) were purchased from Avanti Polar Lipids (Alabaster, USA). Bovine collagen I (5 mg mL^{-1}) (A1064401), phosphate buffer saline (PBS) (10010-023), Dubelcco's Minimum Essential Media (DMEM) (11995065), fetal bovine serum (FBS) (16000044), and penicillin-streptomycin-glutamine 100× (10378016) were purchased from Gibco. The collagen fluorescent dye, succinimidyl (NHS) ester of Alexa Fluor 647 was supplied by Life Technologies. Triton-X 100, 4′,6-diaminodino-2-phenylindole (DAPI), paraformaldehyde (P6148), Tween 20 (P1754), and bovine serum albumin (BSA) (A9647) were procured from Sigma-Aldrich. To stain the nucleus for live cell imaging, NucBlue live readyprobes reagent (Hoechst 33342) (R37605) from ThermoFisher Scientific was purchased. DAPI (D9542) from Sigma-Aldrich was used for nuclei staining. All other reagents used were of analytical grade.

Preparation of Collagen-Encapsulated Nanoliposomes (Lip-Cols) and Characterization: A collagen solution was prepared by mixing bovine tail collagen I with hydrochloride (HCl solution (0.01 M, pH 3) to achieve a concentration of 1 mg mL^{-1}. Prior to use, the collagen solution was filtered through a 200 nm PTFE syringe filter (Whatman, UK) to reduce the size of collagen monomers. The morphology difference before and after filtration was confirmed using AFM (Park Systems, Korea) and Zetasizer Nano ZEN3600 (Malvern Instruments, Malvern, UK) at the Advanced Bio-Interface Core Research Facility, Sogang University.

Lip-Cols were prepared using a method adapted from Lee et al.[43] First, multilamellar liposomes were prepared by mixing DOPC:Chol at a molar ratio of 9.5:0.5 to make a mixture with a total concentration of 5 mg of lipids per milliliter in chloroform. The lipid mixture was then blown dry using N_2 gas and vacuumed for 2 h to remove the solvent completely. For collagen incorporation, the lipid films were hydrated (1:1. v/v) with collagen solution (1 mg mL^{-1}) in pH-3 HCl solution by using vortex mixing at room temperature for 60 min. The lamellarity of the Lip-Cols was reduced by using 5 cycles of freezing in liquid nitrogen and thawing in a water bath at 40 °C to break down the outer bilayers. Finally, Lip-Cols were extruded by using a mini extruder set (Avanti, Inc.) to pass them through a 400-nm membrane filter 11 times. Fluorescently labeled Lip-Cols were made with the same method by adding Top-Chol with 0.32 of the total molar ratio of lipid mixture and rehydrated with collagen solution that had been labeled with NHS Alexa 647. Blank liposomes were prepared using the same method described above. For in vivo formulation, 5% (v/v) propylene glycol was added to the collagen solution for the hydration of lipid films.

The mean hydrodynamic diameter, expressed as intensity, polydispersity index (PDI), and zeta potential of particles were determined using Zetasizer Nano ZEN3600. The measurements were carried out in triplicate at 25 °C for at least three independent preparations. The encapsulation efficiency (EE) of collagen in nanoliposomes was determined using a high-speed centrifugation method with modifications.[44] Lip-Cols were formulated with fluorescent-labeled collagen, and the fluorescent intensity of free and entrapped collagen was measured using a multi-plate reader (EnSpire, Perkin Elmer) to obtain the F_{total}. After centrifugation of Lip-Cols at 20 000 × *g*, 4 °C for 2 h, the free collagen (supernatant) was carefully separated and replaced with an HCl solution. The fluorescent intensity of the resultant solution was measured and presented as $F_{encapsulated}$. The EE of Lip-Cols was calculated with the following equation:

$$EE = \frac{F_{encapsulated}}{F_{total}} \times 100\% \quad (1)$$

The DLC was also determined by the same method, and the percentage of DL was calculated as follows:

$$DLC = \frac{\text{Weight of drug in nanoparticles}}{\text{Weight of nanoparticles}} \times 100\% \quad (2)$$

Electric Field Stimulation, Fibrils Characterization, and ΔpH Measurement: To study the self-assembly of collagen fibrils, 200 µL of Lip-Cols or collagen solution was placed in a home-built reactor made of a 13-mm inner diameter confocal dish with inserted gold-coated electrodes connected to a function generator (Tektronix, Inc., USA). During the electric field stimulation, a 50Ω resistor was connected to the system while applying a sinusoidal wave of 10 Hz frequency, 1 V, and peak-to-peak potential. The self-assembly process was observed under the Confocal Leica SP-8 microscope (Leica Microsystems, Germany) as shown in Figure S2, Supporting Information. The images were analyzed using Image J software and the fluorescence intensity was normalized to the background intensity. No post-imaging process was performed to measure the fluorescence intensity.

The morphological characterization of collagen fibrils from collagen solution or Lip-Cols was observed by TEM—low-voltage electron microscopy (Delong America Inc., USA) at the Advanced Bio-Interface Core Research Facility, Sogang University. After electrification, the sample suspension was tenfold diluted, and a 5-µL drop of the diluted suspension was placed on the TEM grid, the excess was removed with filter paper, and this step was repeated once. The TEM grid with the dropped sample was washed out with 10-µL DIW two times, and the grid was air-dried for 24 h and observed.

To measure the change in ΔpH, a pH Meter LAQUA PH2000 (Horiba Ltd., Japan) was utilized. The pH meter electrode was submerged into a 2-mL solution consisting of HCl solution, collagen, liposome, or Lip-Cols. The solution was then subjected to EF stimulation using electrodes for 1 h with 5-min intervals before and after electrification.

Collagen Structural Analysis: The structural changes in collagen were analyzed using CD and FT-IR spectroscopy to detect any modifications in the secondary structure and functional groups of the protein. The CD spectra were acquired using a Jasco J-815 Spectropolarimeter (Jasco, Inc., Japan). The final concentration of all CD samples was 0.1 mg mL^{-1}. Optically matched quartz cuvettes (0.1 cm path length) were used to load 300 µL of the samples. All ellipticity measurements were performed using the same cuvette for baselines and samples. The FTIR spectral measurements were performed at a resolution of 4 cm^{-1} in the wavenumber range 600–4000 cm^{-1} using the Cary 610 FTIR (Agilent Technologies, Santa Clara, CA, USA) at the Advanced Bio-Interface Core Research Facility, Sogang University.

Cellular Interaction and Collagen Orientation Analysis: The cellular interaction of collagen, NLs, and Lip-Cols in HDF cells was examined using live cell imaging with a confocal microscope. Prior to the experiment, HDF cells were treated with NucBlue to stain their nucleus. A concentration of 50 µg mL^{-1} of fluorescently-labeled collagen-only, liposome-only, or Lip-Cols was directly exposed to the nucleus-stained HDF cells and monitored in real-time. For Lip-Cols with EF group, the electrical stimulation was applied directly to the culture medium as mentioned previously. After 1 h, HDF cells were washed with PBS, replaced with fresh medium, and continued to be observed. The orientation of collagen fibrils was quantified using the directionality plugin Image J software. The orientation of collagen fibrils was measured from the collagen channel and the orientation of cells was measured from the bright-field channel.

Epidermis-Dermis Transwell System: Human keratinocyte (HaCaT) cells and adult HDF cell line were cultured in DMEM medium supplemented with 10% FBS and 1% antibiotics (penicillin-streptomycin) at a temperature of 37 °C with 5% CO_2. Cells were passaged by trypsinization using 0.5% trypsin/ethylenediaminetetraacetic (EDTA) when they reached a confluent state. To evaluate the permeability of Lip-Cols in cell monolayer, a HaCaT cell monolayer was prepared by culturing cells with a density of 1 × 10^5 cell/6.5 mm in the insert of commercially available 24-well transwells (Corning, NY, USA) on polycarbonate membranes with 0.4 µm diameter pores. After the monolayer reached confluency, the upper compartment (insert) was moved to a 24-well cell culture plate made of polystyrene that had been cultured with 1 × 10^5 cell/13 mm HDF cells on a coverslip to form two compartments, where the upper side consisted of HaCaT cell monolayer and the lower side consisted of HDF cells (Figure S5, Supporting Information). Permeability testing was conducted on three transwell membranes by incubating the membranes with a 20 µL mL^{-1} Alexa 647 mixed medium supplemented with 0.5% FBS. After an hour incubation period, the cell medium in the plate well was collected and analyzed using a multi-plate reader. For the Lip-Cols permeability test, the media in the lower compartment was replaced with 0.6 mL solutions of cell media supplemented with 0.5% FBS, and the upper compartment was filled with 0.1 mL cell media solutions supplemented with 0.5% FBS mixed with 150 µg mL^{-1} fluorescently-labeled Lip-Cols or collagen and observed at different time points (0, 2, 4, 8, 16 h). The HDF cells on the coverslip were stained with DAPI and mounted on a glass slide for confocal microscopy imaging with a 40× objective lens after Lip-Cols exposure.

In Vivo Permeability of Labeled Collagen and Lip-Cols: Animal model experiments were conducted in accordance with the approved IACUC protocol (No. IACUCSGU2023_10) by Sogang Univeristy and followed the guidelines outlined in the Guide for the Care and Use of Laboratory Animals of the National Institutes of Health. Female ICR mice aged 7 weeks ($N = 30$) were maintained in a temperature-controlled room (22 °C) at 55% humidity, with a 12-h light/dark cycle. The mice were individually caged for at least 24 h before the experiment. Anesthesia was induced intraperitoneally using 25 mg mL^{-1} of 2,2,2-tribromoethanol (Avertin). The dorsal part of the mice was clean-shaved and designated areas with a surface area of 1 cm^2 were marked. The control area was left untreated, while areas designated for collagen application, with or without EF, were treated with 200 µL of a 0.5 mg mL^{-1} solution of labeled collagen. Similarly, areas designated for Lip-Cols application, with or without EF, were treated with 200 µL of a 0.5 mg mL^{-1} solution of labeled Lip-Cols. Subsequent to 1 h incubation with the respective sample solutions, EF was applied using home-built electrodes. Following a 24-h interval, the dorsal skin was carefully excised for histological examination and total collagen quantification. Histological samples were promptly fixed in 4% paraformaldehyde in PBS and sent to KCFC pathology laboratory (Korea, Seoul) for fluorescence nuclei staining. For total collagen analysis, tissue specimens were snap-frozen in liquid nitrogen and stored at −80 °C until analysis. Upon weighing the tissues, 100 µL of acid-pepsin solution was added, and the samples were gently agitated overnight. Collagen content was assessed using the Sircol Soluble Collagen Assay (Biocolor Ltd., UK) following the manufacturer's guidelines.

To evaluate the permeability of fluorescently labeled collagen and NLs, the Image J software was employed to define regions of interest (ROIs) as 10 µm × 1 µm rectangles. These ROIs were strategically placed to measure fluorescent intensity across the confocal images of tissue samples. The initial reference point was normalized to the outermost layer of the skin and processed into graphs and heatmaps using Origin 2023 software. A total of twenty histological section images were examined for each experimental group. For the assessment of fluorescent intensity in the dermal layer, three points of ROI within the dermal layer were measured across twenty histological sections for each experimental group.

Statistical Analysis: All data were preprocessed to identify outliers, after which data were presented as means ± standard deviations (SDs) or standard error of the mean from at least three independent measurements. Data were analyzed using the one-way Analysis of Variance (ANOVA) followed by Tukey's test, and the level of significance was determined at $*p < 0.05$ by using Origin 2023.

Supporting Information

Supporting Information is available from the Wiley Online Library or from the author.

Acknowledgements

This work was supported by the Basic Research Program (2018R1A6A1A03024940) of the Ministry of Education, the Mid-Career Researcher Program (2019R1A2C2084638), and the Global Research Network Program (2021K1A4A8A02079222) of the Ministry of Science and ICT, Korea. The authors also thank Dr. S. Hong of NCT, Co. for providing insightful discussions that greatly aided the protocol development.

Conflict of Interest

The authors declare no conflict of interest.

Data Availability Statement

The data that support the findings of this study are available in the supplementary material of this article.

Keywords

collagen fibril, electric field, extracellular matrix, nanoliposome

Received: April 9, 2024
Revised: May 14, 2024
Published online: May 31, 2024

[1] M. Zheng, X. Wang, Y. Chen, O. Yue, Z. Bai, B. Cui, H. Jiang, X. Liu, *Adv. Healthcare Mater.* **2023**, *12*, 2202042.
[2] C. Gorzelanny, C. Mess, S. W. Schneider, V. Huck, J. M. Brandner, *Pharmaceutics* **2020**, *12*, 684.
[3] a) J. Zhu, Z. Li, Y. Zou, G. Lu, A. Ronca, U. D'Amora, J. Liang, Y. Fan, X. Zhang, Y. Sun, *J. Leather Sci. Eng.* **2022**, *4*, 30; b) S. Gajbhiye, S. Wairkar, *Biomater. Adv.* **2022**, *142*, 213152.
[4] F. Urdiales-Gálvez, N. E. Delgado, V. Figueiredo, J. V. Lajo-Plaza, M. Mira, A. Moreno, F. Ortíz-Martí, R. del Rio-Reyes, N. Romero-Álvarez, S. R. del Cueto, M. A. Segurado, C. V. Rebenaque, *Aesthetic Plast. Surg.* **2018**, *42*, 498.
[5] L. Chotphruethipong, M. Battino, S. Benjakul, *Food Chem.* **2020**, *328*, 127127.
[6] N. Tiwari, E. R. Osorio-Blanco, A. Sonzogni, D. Esporrín-Ubieto, H. Wang, M. Calderón, *Angew. Chem., Int. Ed.* **2022**, *61*, e202107960.
[7] a) S. M. Mirvakili, R. Langer, *Nat. Electron.* **2021**, *4*, 464; b) D. Ramadon, M. T. C. McCrudden, A. J. Courtenay, R. F. Donnelly, *Drug Delivery Transl. Res.* **2022**, *12*, 758.
[8] S. D. Huelin, H. R. Baker, K. M. Poduska, E. F. S. Merschrod, *Macromolecules* **2007**, *40*, 8440.
[9] X. Cheng, U. A. Gurkan, C. J. Dehen, M. P. Tate, H. W. Hillhouse, G. J. Simpson, O. Akkus, *Biomaterials* **2008**, *29*, 3278.
[10] M. Lei, S. Zhang, H. Zhou, H. Wan, Y. Lu, S. Lin, J. Sun, X. Qu, C. Liu, *ACS Nano* **2022**, *16*, 10632.
[11] a) A. Golberg, S. Khan, V. Belov, K. P. Quinn, H. Albadawi, G. Felix Broelsch, M. T. Watkins, I. Georgakoudi, M. Papisov, M. C. Mihm Jr, W. G. Austen Jr, M. L. Yarmush, *Sci. Rep.* **2015**, *5*, 10187; b) T. C. F. d. Oliveira, S. d. F. S. Rocha, D. G. Ramos, C. G. Ramos, M. V. d. A. Carvalho, M. G. Ramos, *Dermatol. Res. Pract.* **2017**, *2017*, 4146391; c) E. B. Nguyen, J. Wishner, K. Slowinska, *J. Electroanal. Chem.* **2018**, *812*, 265.

[12] S. Morozova, M. Muthukumar, *J. Chem. Phys.* **2018**, *149*, 163333.
[13] M. B. R. Pierre, I. dos Santos Miranda Costa, *Arch. Dermatol. Res.* **2011**, *303*, 607.
[14] M. D. Phan, K. Y. Lee, J. Lee, S. K. Satija, K. Shin, *Langmuir* **2020**, *36*, 7259.
[15] a) A. S. Parmar, M. Joshi, P. L. Nosker, N. F. Hasan, V. Nanda, *Biomolecules* **2013**, *3*, 986; b) O. Lieleg, R. M. Baumgärtel, A. R. Bausch, *Biophys. J.* **2009**, *97*, 1569.
[16] A. Olżyńska, W. Kulig, H. Mikkolainen, T. Czerniak, P. Jurkiewicz, L. Cwiklik, T. Rog, M. Hof, P. Jungwirth, I. Vattulainen, *Langmuir* **2020**, *36*, 10438.
[17] a) I. Bekard, D. E. Dunstan, *Soft Matter* **2014**, *10*, 431; b) L. J. Martin, B. Akhavan, M. M. M. Bilek, *Nat. Commun.* **2018**, *9*, 357.
[18] a) K. Shyh Ming, C. Shwu Jen, H. Chia Che, C. Shu Fen, L. Li-Chun, presented at 2005 IEEE Engineering in Medicine and Biology 27th Annual Conf., Shanghai, January, **2005**; b) R. de la Rica, E. Mendoza, L. W. Chow, K. L. Cloyd, S. Bertazzo, H. C. Watkins, J. A. M. Steele, M. M. Stevens, *Small* **2014**, *10*, 3876.
[19] M. Ammam, *RSC Adv.* **2012**, *2*, 7633.
[20] E. J. Lafarge, P. Muller, A. P. Schroder, E. Zaitseva, J. C. Behrends, C. M. Marques, *Proc. Natl. Acad. Sci. U. S. A.* **2023**, *120*, e2213112120.
[21] L. Wang, H. Lyu, X. Zhang, Y. Xiao, A. Li, Z. Ma, C. Guo, Y. Pei, *Food Hydrocolloids* **2022**, *130*, 107700.
[22] Y. Li, A. Asadi, M. R. Monroe, E. P. Douglas, *Mater. Sci. Eng., R* **2009**, *29*, 1643.
[23] D. Li, Y. Sun, Z. Yang, L. Gu, Y. Chen, H. Zhou, *Joule* **2018**, *2*, 1265.
[24] J. A. Uquillas, O. Akkus, *Ann. Biomed. Eng.* **2012**, *40*, 1641.
[25] S. L. Yuanyuan Zhou, D. Wang, Y. Zhao, X. Lei, *Biosci. J.* **2018**, *34*, 779.
[26] P. Qi, Y. Zhou, D. Wang, Z. He, Z. Li, *RSC Adv.* **2015**, *5*, 87180.
[27] B. de Campos Vidal, M. L. S. Mello, *Micron* **2011**, *42*, 283.
[28] R. Wiens, C. R. Findlay, S. G. Baldwin, L. Kreplak, J. M. Lee, S. P. Veres, K. M. Gough, *Faraday Discuss.* **2016**, *187*, 555.
[29] R. I. Litvinov, D. A. Faizullin, Y. F. Zuev, J. W. Weisel, *Biophys. J.* **2012**, *103*, 1020.
[30] M. Ashoorirad, M. Saviz, A. Fallah, *J. Mol. Liq.* **2020**, *300*, 112344.
[31] a) W. Han, S. Chen, W. Yuan, Q. Fan, J. Tian, X. Wang, L. Chen, X. Zhang, W. Wei, R. Liu, J. Qu, Y. Jiao, R. H. Austin, L. Liu, *Proc. Natl. Acad. Sci. U. S. A.* **2016**, *113*, 11208; b) M. H. Iqbal, F. J. R. Revana, E. Pradel, V. Gribova, K. Mamchaoui, C. Coirault, F. Meyer, F. Boulmedais, *ACS Nano* **2022**, *16*, 20034.
[32] R. Bednarek, *Methods Protoc.* **2022**, *5*, 17.
[33] Y. Ha, Y. Koo, S.-K. Park, G.-E. Kim, H. B. Oh, H. R. Kim, J.-H. Kwon, *RSC Adv.* **2021**, *11*, 32000.
[34] V. V. Artym, *Curr. Protoc. Cell Biol.* **2016**, *70*, 10191.
[35] K. Sakai-Kato, K. Yoshida, K.-i. Izutsu, *Chem. Phys. Lipids* **2019**, *224*, 104726.
[36] D. Montizaan, K. Yang, C. Reker-Smit, A. Salvati, *Nanomedicine* **2020**, *30*, 102300.
[37] M. Li, M. Li, X. Li, W. Shao, X. Pei, R. Dong, H. Ren, L. Jia, S. Li, W. Ma, Y. Zeng, Y. Liu, H. Sun, P. Yu, *Int. J. Nanomed.* **2023**, *18*, 1853.
[38] W. J. Richardson, J. W. Holmes, *Biophys. J.* **2016**, *110*, 2266.
[39] R. Gupta, B. Rai, *Langmuir* **2018**, *34*, 5860.
[40] N. Kis, A. Kovács, M. Budai-Szűcs, G. Erős, E. Csányi, S. Berkó, *J. Drug Delivery Sci. Technol.* **2022**, *69*, 103161.
[41] X. Li, N. Saeidi, M. Villiger, H. Albadawi, J. D. Jones, K. P. Quinn, W. G. Austin Jr, A. Golberg, M. L. Yarmush, *J. Tissue Eng. Regener. Med.* **2018**, *12*, 2309.
[42] Y. Long, H. Wei, J. Li, G. Yao, B. Yu, D. Ni, A. L. F. Gibson, X. Lan, Y. Jiang, W. Cai, X. Wang, *ACS Nano* **2018**, *12*, 12533.
[43] K. Y. Lee, H. T. Nguyen, A. Setiawati, S.-J. Nam, M. Kim, I.-G. Ko, W. H. Jung, K. K. Parker, C.-J. Kim, K. Shin, *Adv. Healthcare Mater.* **2022**, *11*, 2101599.
[44] X.-R. Shao, X.-Q. Wei, S. Zhang, N. Fu, Y.-F. Lin, X.-X. Cai, Q. Peng, *Nanoscale Res. Lett.* **2017**, *12*, 504.